APPENDIX A

"FT-IR EMISSION/TRANSMISSION TOMOGRAPHY OF A COAL FLAME"

Paper Submitted to the 23rd International Symposium of the Combustion Institute, 1990

FT-IR EMISSION/TRANSMISSION TOMOGRAPHY OF A COAL FLAME

J.R. Markham, Y.P. Zhang, R.M. Carangelo, and P.R. Solomon
Advanced Fuel Research, Inc., 87 Church Street, East Hartford, CT 06108

ABSTRACT

Fourier Transform Infrared (FT-IR) Emission/Transmission (E/T) spectroscopy has recently been shown to be a versatile technique for coal combustion diagnostics by allowing for measurements of particle concentrations and temperatures, and gas compositions, concentrations, and temperatures. These measurements are for the ensemble of particles and gases along a line-of-sight in the flame. In this paper, tomographic reconstruction techniques have been applied to line-of-sight FT-IR E/T measurements to derive spectra that correspond to small volumes within a coal flame. From these spectra, spatially resolved point values for species temperature and relative concentrations can be determined. The technique was used to study the combustion of Montana Rosebud subbituminous coal burned in a transparent wall reactor. The coal is injected into the center of an up-flowing preheated air stream to create a stable flame. Values for particle temperature, relative particle density, relative soot concentration, the fraction of ignited particles, the relative radiance intensity, the relative CO_2 concentration and the CO_2 temperature have been obtained as functions of distance from the flame axis and height above the coal injector nozzle. The spectroscopic data are in good agreement with visual observations and thermocouple measurements. The data present a picture of the coal burning in a shrinking annulus which collapses to the center at the tip of the flame. CO_2 temperatures are highest in the rapid burning zone (2300 to 2900 K). The highest particle temperatures in this zone are 1900 to 2000 K, with temperatures up to 2400 K outside the zone.

INTRODUCTION

Better understanding of the coal combustion process would promote more reliable utilization of coals having a diversity of characteristics and would enable improved combustion systems to be designed and developed. Among the processes which are the least well understood and predicted are: ignition, soot formation, swelling, char reactivity, and ash formation. Recently, Fourier Transform Infrared (FT-IR) Emission/Transmission (E/T) spectroscopy was applied to a laboratory scale coal flame to determine ignition, soot formation, particle temperature, particle concentrations, gas temperatures and gas concentrations for a number of coals varying in rank from lignite to low volatile bituminous.[1] Chars and demineralized coals were also included in this study. The study demonstrated that the FT-IR E/T technique is a versatile diagnostic for studying coal combustion. However, it suffers from being a line-of-sight technique.

To correct this shortcoming, tomography techniques have been applied to both the FT-IR emission and transmission spectra to obtain spatially resolved spectra. This method has recently been applied to a stable, well defined co-annular laminar ethylene diffusion flame.[2,3] From the spatially resolved spectra, point values for species temperature and relative concentrations were determined for CO_2, H_2O, alkanes, alkenes, alkynes, and soot. The CO_2 and H_2O temperatures were found to be in good agreement with measurements performed on the same flame by coherent-anti-Raman spectra (CARS),[4] and the soot concentrations were in good agreement with soot concentrations determined by laser scattering.[5]

This paper describes the application of FT-IR E/T tomography to a coal flame produced in a transparent wall reactor. From these spectra, spatially resolved point values have been obtained for particle temperature, relative particle density, relative soot

concentration, the fraction of ignited particles, the relative radiance intensity, the relative CO_2 concentration and the CO_2 temperature.

EXPERIMENTAL

Apparatus

The Transparent Wall Reactor (TWR) facility has been described previously.[1] The coal is injected upwards into a center of a 10 cm diameter upward flowing preheated air stream in the center of a 20 cm diameter x 70 cm tall glass enclosure. Figure 1 shows the temperature in the stream as a function of position measured with a thermocouple in the absence of coal. The preheated air stream provides a stable hot environment for the coal up to a height of 30 cm. Critical to the measurements is the flame stability which relies on a steady particle feeding system. Our feeding system employs mechanical vibration to displace and entrain particles into a carrier gas. Improvements in the vibration system have resulted in a flame which is very stable in shape and position except for the ignition point where verticle fluctuations of $\pm$ 5 mm are observed.

The enclosure has movable KBr windows to allow access to the flame by the FT-IR spectrometer (a modified Nicolet 20SX). As discussed in Ref. 6, emission measurements are made by directing the radiation emitted by the hot sample stream through an interferometer to an "emission" detector. Transmission measurements are made by replacing this detector with a high intensity globar source which, after passing through the interferometer, is directed through the sample area to a "transmission" detector. The emission and transmission measurements are made along the same 1 mm wide by 4 mm high optical path defined with apertures. With this optical geometry, parallel line-of-sight emission and transmission spectra were collected across the coal stream at 1 mm increments along the radius.

MCT infrared detectors were used for both emission and transmission measurements. It is important to avoid possible saturation of the transmission detector due to the direct impingement of flame radiation on the detector. Two methods were employed to verify that this did not occur: 1) reproducible line-of-sight attenuation was observed when the detector was apertured to reduce the overall intensity, and 2) the same intensity was observed in a region of the spectrum that was totally blocked (achieved by flooding the beam path with CO_2) in both the flame on and flame off conditions. Different intensities would indicate saturation.

Sample

The sample used in this experiment was a sieved fraction (200 x 325 mesh) of dry Montana Rosebud subbituminous coal. The characteristics of this coal has been published previously.[1,7] The current sample has an 11% ash content. The coal was fed into the TWR at a rate of 1.6 g/min.

Coal Flame

The flame generated from this coal is shown in Fig. 2 and reproduces the flame analyzed previously by line-of-sight FT-IR E/T measurements.[1] Figure 2a presents a view of the entire length of the flame. Below the ignition point, a few particles that are in the outer edge of the stream (closest to the hot gas) are observed to ignite. At 10 cm the flame ignites. Also indicated is the extent of the coal weight loss at several locations above the nozzle. The particle stream was collected for these determinations with a 1.6 cm diameter water cooled extractor that adds cold helium gas to the hot stream to drop the temperature below 350°C as it is aspirated to a cyclone separator. Percent burnout was determined by

ash tracer with a thermogravimetric analyzer.

A weight loss of 43.2% (DAF) was observed for material collected at the ignition point. TGA analysis on this char indicated that it contains essentially no remaining volatile matter. All of the particles have reached a temperature to completely devolatilize but not significantly burn at this point in the TWR, based on the starting material's volatile content of 42.8% (DAF).[1]

SEM photographs were made of collected char. At ignition, most particles are of the same dimensions as before ignition but a few particles are larger (presumably swollen) and some are smaller (possibly fragmented).

Figures 2b and 2c show close-up photographs of the flame taken with 1/250 sec and 1/2000 sec exposures, respectively. The photos indicate the structure of the flame, with the highest density of ignited particle shrinking from the edge to the center-line with increasing height above the nozzle. The positions where the FT-IR tomographic slices were measured are also indicated. The photographs show the relatively laminar appearance of the flame (Figs. 2a and 2b) while some non-uniformity can be seen along the center line in Fig. 2c. The steadiness in the flame is also indicated by reproducibility of consecutive spectroscopic measurements. Typically line-of-sight measurements deviate by less than 10%. Multiple measurements are performed to average out these deviations.

Measurements were made of the particle velocities by measuring the length of tracks recorded with a video camera. The results are presented in Fig. 3 for both combustion and pyrolysis conditions. For pyrolysis conditions, sufficient air was added to make a few particles ignite so that they could be viewed. The figure shows the velocities increasing to the hot gas velocity for pyrolysis and above the hot gas velocity for combustion. The video pictures were also analyzed to determine the relative particle density as a function of position. Below the ignition region, scattering from a He-Ne laser was used to determine the width of the particle stream.

ANALYSIS

Line-of-Sight FT-IR E/T Measurements

The analysis for the line-of-sight FT-IR E/T measurement pertaining to multi-phase reacting streams has been presented previously.[1,5,8-10] It is an extension of the emission/transmission method applied to gases and soot.[11-14]

For a medium containing gases and soot with absorption coefficients α^g_ν and α^s_ν and particles of geometrical cross-sections A at a density of N particles cm^{-3}, the measured transmittance, τ_ν, is given by

$$\tau_\nu = \exp(-(\alpha^s_\nu + \alpha^g_\nu + NAF^t_\nu)\, L) \qquad (1)$$

where F^t_ν is the ratio of the total cross-section (extinction) to the geometrical cross-section, and L is the path length. The relative concentrations of individual gas species, (related to α^g_ν), soot (related to α^s_ν) and particles (related to NAF_ν) are determined from the regions of the spectra which can be uniquely related to the individual species.

From the radiance R_ν, the normalized radiance $R^n_\nu = R_\nu/(1-\tau)$ is obtained,

$$R^n_\nu = \frac{\alpha^s_\nu R^b_\nu(T_s) + \alpha^g_\nu R^b_\nu(T_g) + NA\,\epsilon_\nu\, R^b_\nu(T_p) + NAF^{s'}_\nu R^b_\nu(T_w)}{\alpha^s_\nu + \alpha^g_\nu + NAF^t_\nu} \qquad (2)$$

where $R^b_\nu(T_g)$, $R^b_\nu(T_s)$, $R^b_\nu(T_p)$ and $R^b_\nu(T_w)$ are the black-body emission spectra at the temperatures T_g, T_s, T_p, and T_w of the gas, soot, particle, and wall, respectively. ϵ_ν is the particle's spectral emittance and $F^{s'}_\nu$ is the cross-section for scattering radiation into the spectrometer. $F^{s'}_\nu$ is taken as negligible in this analysis because the experiment is

performed with room temperature walls and the small diameter of the flame was chosen so that very little scattered radiation from other parts of the flame can enter the spectrometer. The temperatures for individual components are obtained from the normalized radiance as discussed in Refs. 1,6,8-10.

FT-IR E/T Tomography

The reconstruction of spatially resolved FT-IR spectra from multiple line-of-sight spectra has been described in detail elsewhere.[2,3] We have employed the Fourier image reconstruction technique[15] which is capable of handling data from systems of arbitrary shape. Our flame, however, was cylindrically symmetric.

In transmission tomography the projections are of absorbance = $\log_{10}\tau$. The program published by Shepp and Logan was adapted for this work[15] by applying the reconstruction one wavelength at a time.

In spectral regions for which Beer's Law applies, the two-dimensional image reconstructed from line-of-sight absorbance measurements leads to the determination of the spatial dependence of absorbance, and hence relative concentration. Relative concentration can be converted to absolute concentration if appropriate calibration measurements are made.

A straight-forward application of the reconstruction technique to radiance spectra is not possible, because of self-absorption in the sample. In the case of small absorbance encountered in this work (percent transmission > 80%), an emission measurement can be directly corrected by an absorption measurement made along the same path. A self-absorption correction corresponding to that used by Freeman and Katz was employed for the thin sample studied.[16] The Fourier reconstruction program can be applied directly to the

emission thus corrected, to obtain local radiances. These are then converted to normalized radiance and the analysis proceeds as for the line-of-sight spectrum.

Examples of local radiance, transmission and normalized radiance spectra are shown in Figs. 4a, 4b, and 4d. The tomographic reconstruction process enhances noise in data, relative to that in the unprocessed data. In this work the data were smoothed by co-adding data from eight adjacent wavenumber bands. This results in degraded resolution from the 8 cm^{-1} used, although the resolution was still sufficient to quantitatively measure the gas species. The results of the reconstruction were consistent in that the summed absorbance and radiance across the flame diameter agreed with the measured line-of-sight absorbance and radiance, as can be seen in Fig. 4c for absorbance.

In each local absorbance spectrum, characteristic line features associated with carbon dioxide, the major gaseous component within the flame, can be identified (Fig. 4a). The area of this component line above the solid phase continuum was measured to derive the local relative concentration of CO_2. Water is observed in the spectrum but not resolved well enough for quantitative determinations. The shape and amplitude of the solid phase continuum can be analyzed to derive the local relative concentrations of particles or mixtures of particles and soot as described in Ref. 1.

In like manner, each species can be identified in the local radiance spectra (Fig. 4b). The particle/soot emission continuum is subtracted to determine the radiance contribution from CO_2. The corrected local emission and transmission values can then be employed to determine local species temperatures.

Figure 4d shows a normalized radiance spectrum calculated by the local radiance and transmission values. The local particle temperatures are obtained by comparing the normalized radiance to theoretical black-body curves, which are "fit" to the data in regions where the solid phase continuum is not influenced by the gas phase species. Overlayed is a gray-body fit to determine particle temperature. As described in Ref. 1, the black-body

multiplier used for each case is the constant fraction of the theoretical black-body which produces the best match in shape and amplitude to the experimental data. For a completely homogeneous sample of gray-body particles, M would be the particle's emissivity. For this case, some particles may be unignited, or ash particles may be present at a much lower temperature and have a very low emittance. The multiplier than approximates the fraction of particles ignited in each local area times their emissivity.

RESULTS

Tomographic reconstruction has been applied to four sets of 21 parallel line-of-sight E/T measurements, at heights of 6, 12, 16, and 20 cm above the nozzle. One set of measurements was for a region below the visually observed ignition point, where particle heat-up and devolatilization were occurring; one set of measurements was just above ignition and the two others were further up in the flame. The data are presented in Figs. 5 to 7.

Figure 5a presents the height of the continuum blockage determined from the transmittance spectra as percent blockage of the incident IR beam. The total blockage is divided into particles and soot as described in Ref. 1. Soot is observed to appear at ignition as inferred by the change in shape of the continuum, from sloping (particles) to flat (soot and particles). Below the ignition (6 cm above the nozzle) there are particles only (no soot) confined to a radius of about 6 mm. This is in agreement with the boundaries as determined using the He-Ne laser. The multiplier, M (the product of emissivity times the fraction of ignited particles) in Fig. 5b shows a few particles (up to 10%) have ignited at the edge of the coal stream. Such ignited particles can also be seen in Figs. 2a and 2c.

Just above ignition (12 cm above the nozzle), the particles appear to be forced inward into a more dense central stream at the same time that some particles are spread outward. The spreading of the stream is confirmed by the video camera. The outward velocity of

particles can also be seen in Fig. 2b. This spreading is consistent with the location of the ignition zone centered at about 4.75 mm radius, indicated by the 0.5 M value in Fig. 5b (i.e., half the particles ignite) as well as the high level of ignited material shown in Fig. 6a, the high radiance in Fig. 6b and the high CO_2 temperature in Fig. 7a. The increase in gas volume in this zone must create pressure to compress the stream inward and expand the stream outward. The total blockage determined by integrating the blockage times area is shown in Fig. 5a. The integrated particle blockage is increased from 1.0 (by definition) at 6 cm to 1.5 at 12 cm. This suggests that the devolatilization which appears complete at this point may swell or fragment the particles to increase the blockage.

At 16 cm the particle blockage is reduced (0.8) as the material burns out (Fig. 5a) and the ignition zone moves inward (Figs. 5b, 6, and 7a).

At 20 cm, the blockage appears to go back up due to the increased blockage at radiuses above 4 mm. It is likely that the blockage at the edge of the stream is now due to ash as it is no longer luminous. The ignition zone has now moved to the center of the stream.

Figure 6 presents the amount of burning material determined from: a) the multiplier M (Fig. 5b) times the total blockage (Fig. 5a), and b) the total local radiance determined at 4500 cm^{-1} from the local R_ν spectra. These two determinations are in reasonable agreement. Both show the ignition zone decreasing from a radius of about 4.25 mm at 12 cm height to the axis at 20 cm height. The high value of radiance along the center line at 12 cm and 16 cm results from the very high values of the particle density even though M is low. The regions of high radiance determined spectroscopically agree with visual and photographic determinations of the bright ignition zone and the total luminous zone as shown on the figure.

Figure 7a presents the temperature of CO_2 (dashed line) and total continuum, both particles and soot (solid line). Also presented are measurements with a Pt + PtRh

thermocouple obtained at several points in the flame. The thermocouple temperature has been radiation corrected using a 0.9 emissivity because of the soot and ash coatings which developed on the surface. These readings are in reasonable agreement with the CO_2 temperatures. The particles have a relatively constant temperature between 1900 K and 2000 K in the ignition zone. Higher Temperatures (2200 to 2400 K) are, however, observed outside these zones. The higher temperature at large radius is understandable as due to a higher level of O_2. The higher temperature at smaller radius for 12 cm matches the CO_2 temperature, but the higher temperature along the center line at 16 cm is puzzling. Note that prior to ignition, the ignited particles are only at 1700 K, but here, the ambient temperature is only 1500 to 1600 K as determined from the CO_2 temperature.

The CO_2 temperatures are also presented in Fig. 6a (dashed line). The maximum CO_2 temperatures (2300 to 2900 K) occur in the regions of high particle radiance where the maximum combustion is occurring. These temperatures are 400 - 1000K hotter than the particles in the same region suggesting that CO is burning to CO_2 away from the particles. CO_2 temperatures are generally lower (below 2000 K) and are closer to the particle temperatures away from the ignition zone. The exception is the center at 16 cm which, as mentioned above, is puzzling. At 20 cm the CO_2 and particle temperatures are within 100 K except along the axis (the ignition zone) where the CO_2 temperature is hotter.

The CO_2 concentrations are presented in Fig. 6b. The relative concentration of CO_2 is determined from the area of the absorbance band. Below ignition the CO_2 concentration is very small. Above ignition the CO_2 level jumps drastically and spreads with increasing height. The shape of the CO_2 concentration at 12 cm is inverse to the shape of the CO_2 temperature and is most likely due to the variation in CO_2 density with temperature.

CONCLUSIONS

Tomographic reconstruction techniques have been applied to FT-IR E/T measurements to derive local values for species temperatures and concentrations within a laboratory scale coal flame. Values for particle temperature, relative particle density, relative soot concentration, the fraction of ignited particles, the relative radiance intensity, the relative CO_2 concentration and the CO_2 temperature have been obtained as functions of distance from the flame axis and height above the coal injector nozzle. The spectroscopic data are in good agreement with visual observations and thermocouple measurements. The data present a picture of the coal burning in a shrinking annulus which collapses to the center at the tip of the flame. CO_2 temperatures are highest in the rapid burning zone (2300 to 2900 K). The highest particle temperatures in this zone are 1900 to 2000 K, with temperatures up to 2400 K outside the zone.

ACKNOWLEDGEMENT

This work was supported under the U.S. Department of Energy, Morgantown Energy Technology Center Contract No. DE-AC21-86MC23075. Richard Johnson is the Project Manager for this program.

REFERENCES

1. Solomon, P.R., Chien, P.L., Carangelo, R.M., Best, P.E., and Markham, J.R.: Twenty-Second Symposium (International) on Combustion, p. 211, The Combustion Institute, (1988).

2. Chien, P.L., Best, P.E., Carangelo, R.M., and Solomon, P.R., "Tomographic Reconstruction of Fourier Transformed Infrared (FT-IR) Spectra at Points within a Coannular Flame", poster session 22nd Symposium (Int) on Combustion, Seattle, Washington, DC, (Aug. 1988).

3. Best, P.E., Chien, P.L., Carangelo, R.M., Solomon, P.R., Danchak, M. and Ilovici, I.: "Tomographic Reconstruction of FT-IR Emission and Transmission Spectra in a Sooting Laminar Diffusion Flame: Species Concentrations and Temperatures", Combustion and Flame, submitted for publication (1989).

4. Boedeker, L.R., and Dobbs, G.M., Comb. Sci. Technol., 46:301, (1986).

5. Santoro, R.J., Semerjian, H.G., and Dobbins, R.A., Combustion and Flame, 51:203, (1983).

6. Best, P.E., Carangelo, R.M., and Solomon, P.R.: Combustion and Flame 66, 47, (1986).

7. Serio, M.A., Hamblen, D.G., Markham, J.R., and Solomon, P.R.: Energy & Fuel, 1, 138, (1987).

8. Solomon, P.R., Carangelo, R.M., Best, P.E., Markham, J.R., and Hamblen, D.G.: Twenty-first Symposium (International) on Combustion, p. 437, The Combustion Institute, (1987).

9. Solomon, P.R., Best, P.E., Carangelo, R.M., Markham, J.R., Chien, P.L., Santoro, R.J., and Semerjian, H.G.: Twenty-first Symposium (International) on Combustion, p. 1763, The Combustion Institute, (1987).

10. Solomon, P.R., Carangelo, R.M., Best, P.E., Markham, J.R., and Hamblen, D.G.: Fuel 66, 897, (1987).

11. Altenkirch, R.A., Mackowski, D.W., Peck, R.E., and Tong, T.W.: Comb. Sci. Tech. 41, 327, (1984).

12. Tourin, R.H.: Spectroscopic Gas Temperature Measurement, Elsevier, NY, (1966).

13. Limbaugh, C.C.: Infrared Methods for Gaseous Measurement: Theory and Practice, (J. Wormhoudt, Ed.), Marcell Dekker, NY, (1985).

14. Vervisch, P. and Coppalle, A.: Combustion and Flame 52, 127, (1983).

15. Shepp, L.A. and Logan, B.F.: IEEE Trans. Nucl. Science, NS-21, (1974).

16. Freeman, M.P. and Katz, S.J.: Optical Society of Am., 50, (8), 826, (1960).

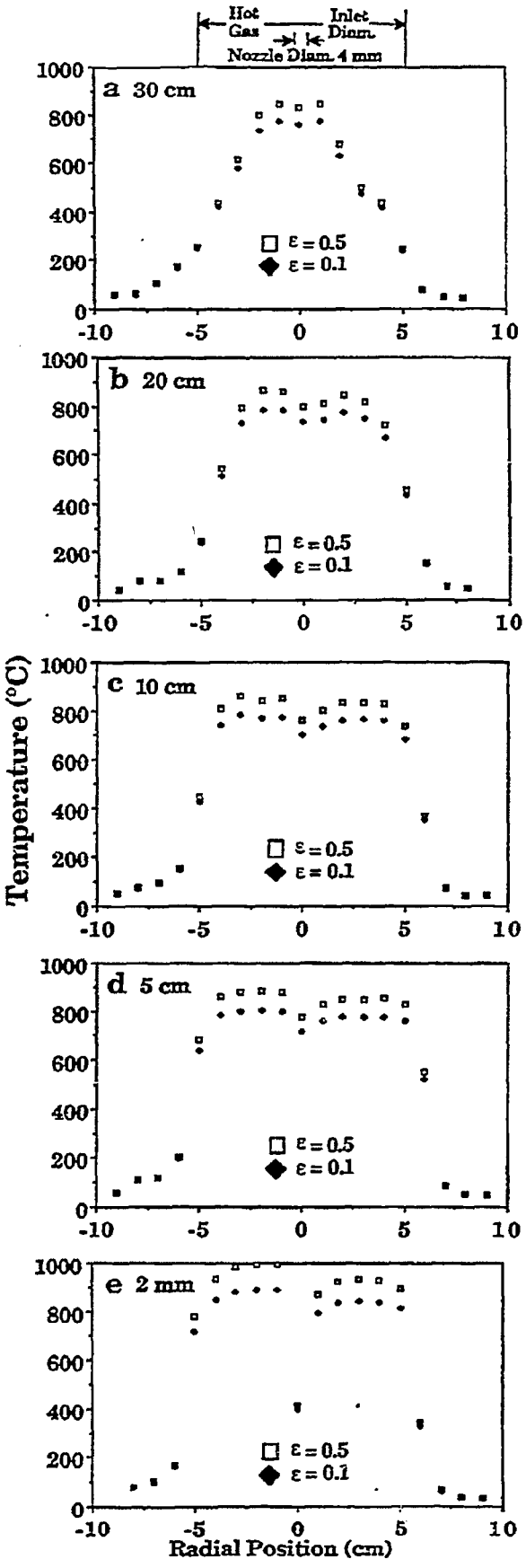

Figure 1. Radial Gas Temperature Profile in the TWR, No Coal Case. ε Represents the Surface Emissivity used to Correct the Type K Thermocouple Measurements for Radiation Loss.

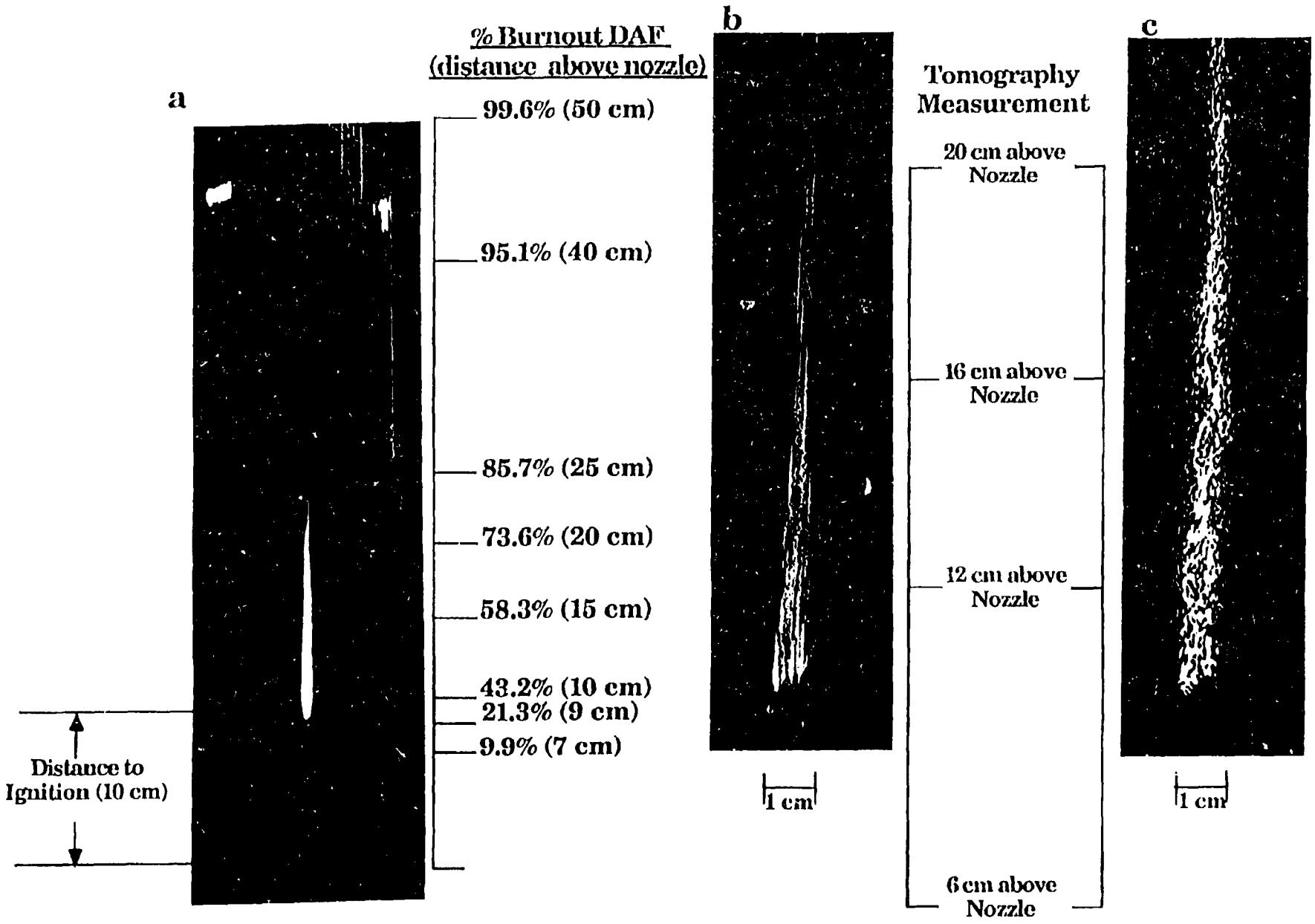

Figure 2. Photographs of Coal Flame in the TWR from Rosebud Subbituminous Coal. a) Flame with% Burnout Values at Indicated Height from Nozzle, b) Long Film Exposure and c) Short Film Exposure Close-ups to Show Density Variation of Ignited Particles Through the Flame. Position of FT-IR Tomographic Measurements are also Indicated.

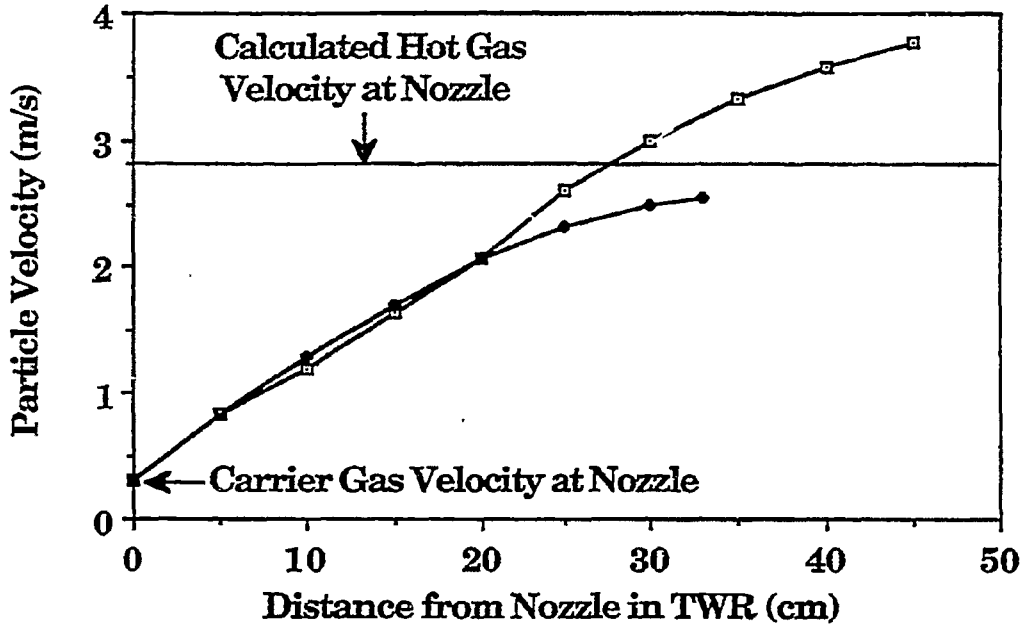

Figure 3. Particle Velocity in the TWR for Pyrolysis (◆) and Combustion (⊡) Conditions

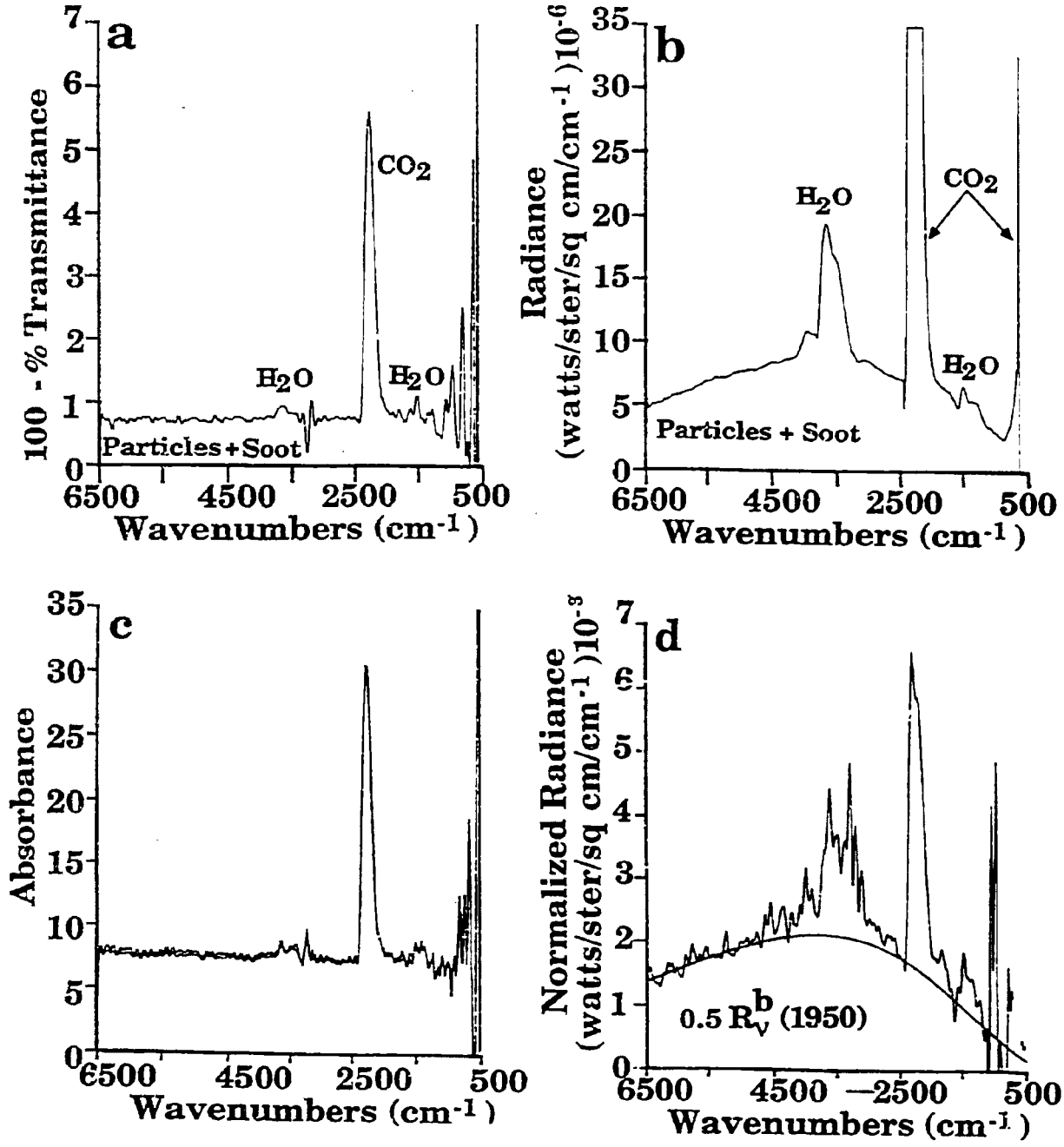

Figure 4. Results of Fourier Reconstruction of the IR Spectra of a Rosebud Coal Flame in the TWR. a) 100-% Transmittance and b) Radiance Measurement at a Radial Position 4mm from the Axis and 2cm Above Ignition. c) Summed Reconstruction of Absorbance Across the Flame Diameter Compared to Line-of-Sight Absorbance. d) Normalized Local Radiance Spectrum with Temperature Determined for the Solid Continuum.

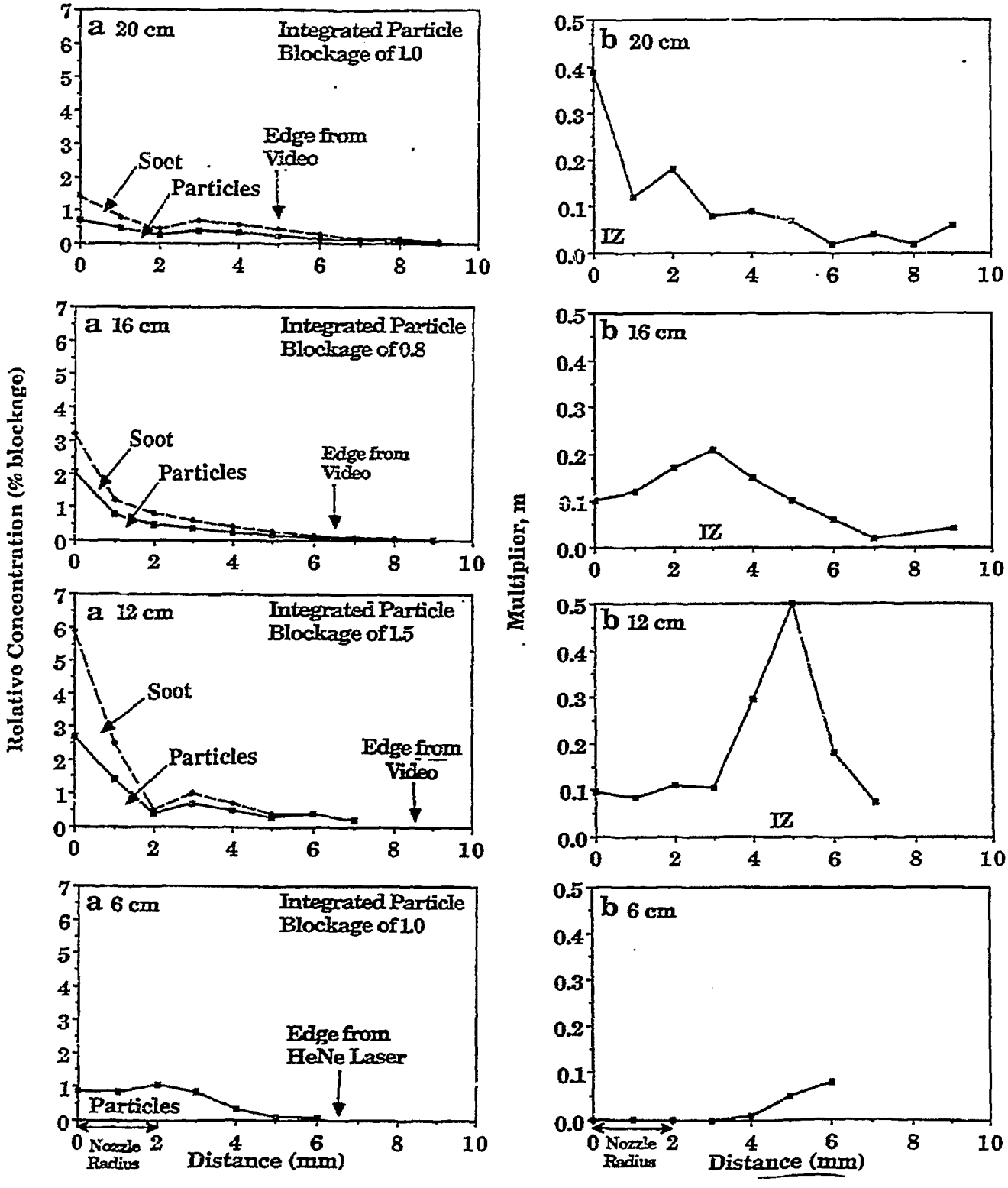

Figure 5. Radial Distributions of a) Particle Concentration and Total (Particle + Soot) Concentration, and b) Multiplier (Black-body Intensity) used for Temperature Determinations at Indicated Distances above the Nozzle for a Rosebud Coal Flame in the TWR. The Region in which the Multiplier, M is a Maximum is Designated by IZ (the Ignition Zone). The Arrows in a) Define the Edge of the Particle Stream Measured with the Video Camera or HeNe Laser.

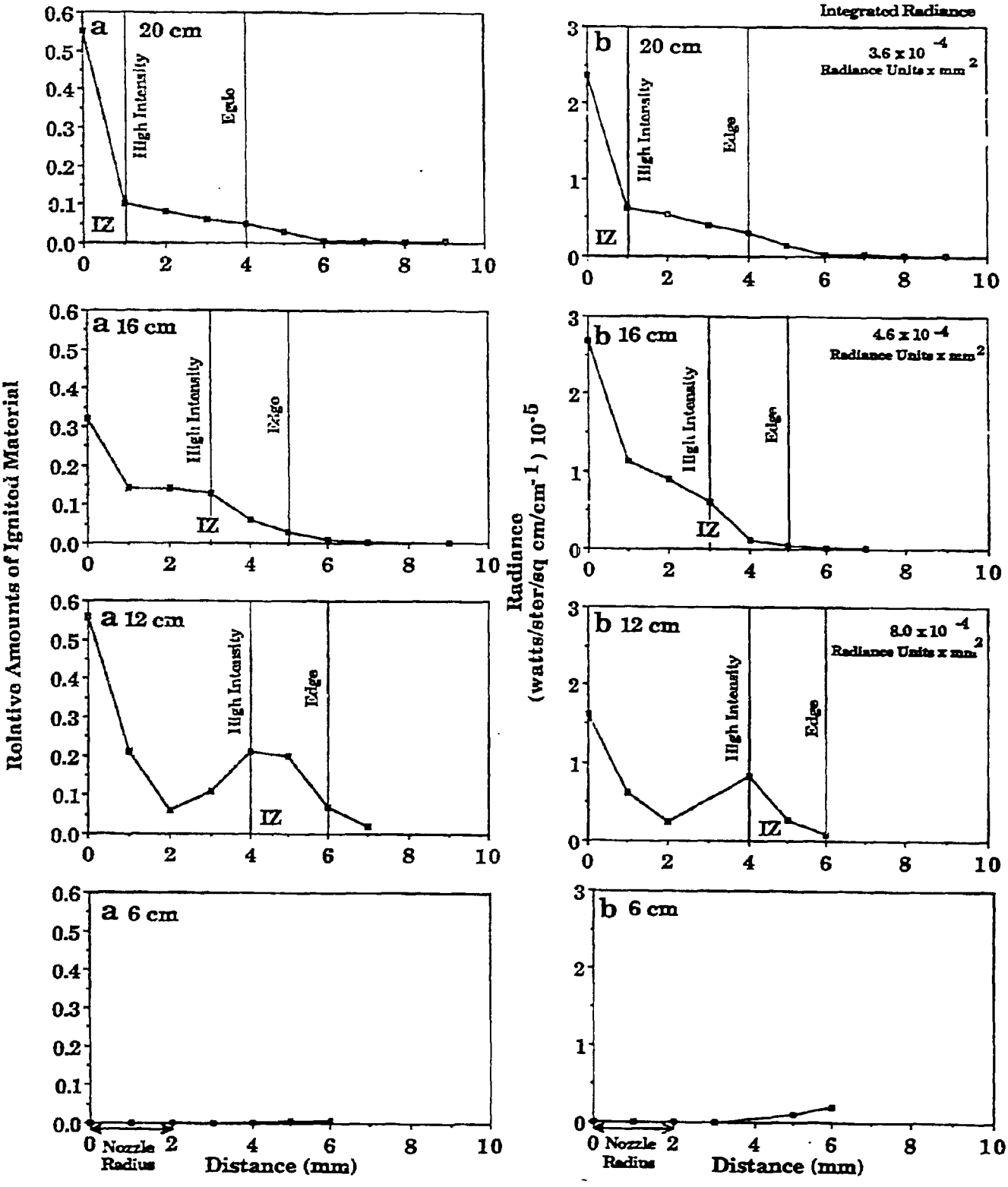

Figure 6. Radial Distributions of a) Relative Amounts of Ignited Material, and b) Radiance Level Measured 4500 cm-1, and at Indicated Distances above the Nozzle for a Rosebud Coal Flame in the TWR. The Ignition Zone (IZ), where the Multiplier, M is at a Maximum and the Edges of Low Intensity and High Intensity Burning Regions are Indicated. Integrated Radial Radiance is also shown in b.

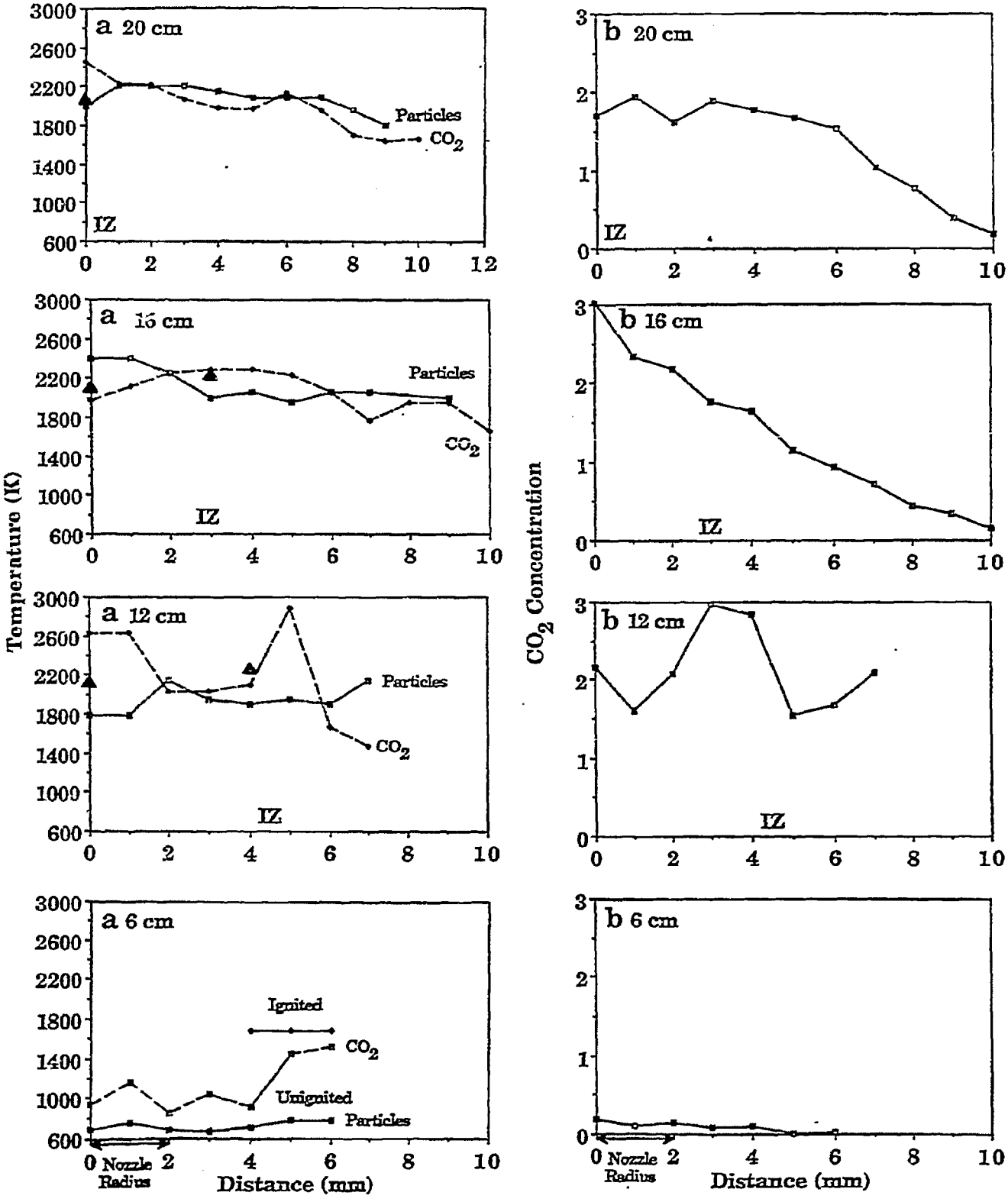

Figure 7. Radial Distributions of a) Particle (solid) and CO2 (dashed) Temperature, and b) CO2 Concentration at Indicated Distances above the Nozzle for a Rosebud Coal Flame in the TWR. Thermocouple Measurements, ▲ are indicated in a) along the Center Axis and at the Edge of the Ignition Zone (IZ), where the Multiplier, M is a Maximum.